Experimental Techniques
https://doi.org/10.1007/s40799-022-00596-z

S.I. : COMPUTATIONS & EXPERIMENTS ON DYNAMICS OF COMPLEX FLUID & STRUCTURE

Analysis of Natural Convection and Radiation from a Solid Rod Under Vacuum Conditions with the Aiding of ANFIS

Imad A. Kheioon[1] · Khalid B. Saleem[1] · Hussein S. Sultan[1]

Received: 15 April 2022 / Accepted: 20 June 2022

Abstract

The present paper represents an experimental and theoretical study of the characteristics of natural convection and radiation heat transfer from a solid cylindrical rod inside a closed vessel under vacuum conditions. The effect of vacuum pressure on the heat transfer rates from the heating element by convection and radiation is clarified. The experimental results are used for Artificial Neural Network (ANN) training which is employed in the Adaptive Neuro Fuzzy Inference System (ANFIS) scheme to predict the heat transfer characteristics. The heat transfer predictions are performed for the solid rod under numerous heat fluxes for each vacuum pressure and the computed outcomes are compared with that predicted from the ANFIS. Outcomes indicated that for a constant heat flux, the convection heat transfer decrease with the reduction in pressure inside the vessel, while the radiation heat transfer will increase. Three methods of ANFIS are deemed in this work; grid partition, subtractive clustering and fuzzy C-mean clustering (FCM). However, the three methods appear an adequate fitting with the experimental data due to the high ability of these schemes at formulating input-output relations. A comparison with conventional correlation for the Nusselt number (Nu) has been implemented which proved the effectiveness and robustness of artificial intelligence in the generation of a direct relation between the effective parameters and the objective functions. Also, the main factors of ANFIS such as the number of membership functions (MFs), the number of clusters and the radius of clusters have been optimized to reach best performance.

Keywords Natural convection · ANFIS · Solid rod · Radiation · Vacuum

Nomenclature

A_s	Bar Surface area (m^2).
C_p	Specific heat (J kg^{-1} K^{-1}).
d	Bar diameter (m).
g	Gravity acceleration (m s^{-2}).
Gr	Grashoff number.
h	Overall coefficient of heat transfer (W m^{-2} K^{-1}).
I	Current (Amp).
k	Thermal conductivity (W m^{-1} K^{-1}).
Nu	Nusselt number.
Nu_{emp}	Empirical Nusselt number.
P	Pressure (Pa).
Pr	Prandtl number.
Q	Total heat transmitted (W).
Q_c	Heat transfer by conduction (W).
Q_r	Heat transfer by radiation (W).
Q_S	Supplied energy (W).
R	Gas constant (J $kg^{-1}K^{-1}$).
T	Temperature (K).
V	Voltage (Volt).

Greek Symbols

β	Thermal expansion coefficient (K^{-1}).
ρ	Air density (kg m^{-3}).
θ_s	Surface temperature difference (K).
σ	Stefan Boltzman constant ($Wm^{-2}K^{-4}$).
μ	Dynamic viscosity (kg $m^{-1}s^{-1}$).

Subscript

a	Air.
m	Mean.
s	Surface.

Imad A. Kheioon
imad.kheioon@uobasrah.edu.iq

✉ Khalid B. Saleem
khalid.saleem@uobasrah.edu.iq

Hussein S. Sultan
hussein.sultan@uobasrah.edu.iq

[1] Department of Mechanical Engineering, College of Engineering, University of Basrah, Basrah, Iraq

Published online: 07 July 2022

Introduction

Free convective transfer of heat from a horizontal cylinder is used in countless industrial applications, including boilers, heat exchangers, and systems of air-conditioning. This subject encounter great interest from several researchers who investigated it numerically and experimentally utilizing various cylinder configurations under numerous conditions and proposed for that many several correlations. Ashjaee et al. [1] and Hayati et al. [2] adopted the ANN to evaluate laminar free convection heat transfer coefficient from an isothermal horizontal cylinder of elliptical cross-section located between two adiabatic walls. The input parameters are based on their experimental work such as tube axis ratio, wall spacing and Rayleigh number (Ra), while the mean Nusselt number (Nu_m) is deemed as the output parameter. Their results noted that the values of the predicted Nu_m with the ANN method are in very good agreement with their experimental data. Atayılmaz and Teke [3] and Atayılmaz [4] did numerical and experimental investigations for the natural convection from a horizontal cylinder heated with a heat flux under numerous environmental temperatures. They utilized ANSYS FLUENT code which adopts the finite volume technique in their numerical simulations. They proposed a correlation for the Nu_m over the cylinder based on the experimental data. Their findings clarified that Nu_m increase with increasing Ra, also they noted that the obtained temperature distributions from numerical simulations were very close to the experimental data. Atayılmaz et al. [5] developed a generalized neural network model to analyze the transfer of heat from horizontal cylinder by natural convection. They utilized the three-layer network for the computations and selected the input parameters as: diameter of cylinder, ambient and cylinder surface temperatures. The objective factor of that study was the Nusselt number (Nu). It can be observed that with a mean relative error of about 2.5%, the trained network provided very best results as compared with that obtained from the correlations. A comparison was implemented between the neural results and correlation results for the Nu_m on the whole cylinder which had appeared in a reasonable agreement. The ANN models considered by Amiri et al. [6] were used to portend natural convection from horizontal arrays of isothermal cylinders arranged vertically and obliquely. They looked at how the average heat transmission from the arrays was affected by the ratios of vertical and horizontal separations' spacing to the cylinder diameter, and Ra. In order to train the ANN, they used the Levenberg-Marquardt back propagation algorithm (LMA). They found that the training and test data had mean relative errors of 0.027% and 0.482%, accordingly, which shows a good consistency between the experimental and predicted results. Tahavvor and Yaghoubi [7] employed ANN to predict the free convective transfer of heat from a column of cold horizontal circular cylinders with monotonic surface temperature. In order to depict the conduct of flow and temperature fields, they developed the Multi-Layer Perceptron (MLP) network, and then broad this behavior to forecast the fields of temperature and flow regardless of Ra value. They stated that the resilient back-propagation algorithm is the best algorithm concerning the faster training method. Saravanakumar et al. [8] applied the ANN to predict the outlet air collector temperature in a solar air heating system (SAHS). Their study focused on determining the act of ANN procedure. They made a comparison between the evaluated and experimental outcomes and clarified that the suggested ANN model is a suitable method for SAHS parameters with acceptable tolerance. Kayaci et al. [9] employed the ANN to determine the physical properties of TiO_2 nanofluids flowing through several micro-fin tubes. They validated their study with a numerical simulation via ANSYS CFD code. Their finding showed that the heat transfer coefficient was slightly augmented by enlarging the nanofluid particles' loading and the CFD code represents a beneficial tool that compensates for the need for experiments. Zainuddin et al. [10] examined the impact of radiation on free convection on a fixed heated horizontal cylinder immersed in a stationary fluid. They implemented the finite difference method to solve the governing equations. They deemed the influence of several parameters on the temperature and velocity profiles such as radiation parameter, heat production parameter and the Prandtl number. Their findings indicate that increasing the radiation parameter results in an increase in the velocity and temperature profiles, as well as local heat transfer rate and the coefficient of local skin friction. A horizontal heated cylinder with and without confining was inspected by Sebastian and Shine [11] for laminar natural convective flow. They adopted the finite volume formulation in the computations and verify the obtained results with experimental data. For a scope of Ra, aspect ratio, and distance between the confinement and the cylinder, the bottom and top sides of the considered structure were studied to determine the effect of confinement. They clarified that at the above surface, the increment in Nu mainly relies upon the region of the taken side. Dey et al. [12, 13] and Das and Dey [14] examined force convective transient flow passing square and circular cylinders. They deemed the square cylinder has rounded corner edges, while there was a copper-water nanofluid flowing over the circular cylinder. They adopted both the ANN and gene expression programming (GEP) to evaluate the heat transmission and flow features. They utilized the

numerical data obtained from ANSYS FLUENT to train the ANN and GEP models. They observed that the mixed convective flow features are predicted properly and correctly by utilizing the back-propagation ANN and GEP, also they elucidated that the data obtained from these schemes are faster that obtained from the regular CFD approach. Kamble [15] examined the heat transmission from horizontal tube bundles inundated in a gas fluidized bed of large particles utilizing ANN. They took into account the impact of numerous parameters in the ANN modeling. They utilized both feed-forward network with back propagation structure in the Levenberg–Marquardt's learning rule in the ANN approach. Their findings were in good accordance with both that obtained from experiments and data from correlations. Ricardo et al. [16] adopted ANN to analyse the convective heat transmission amount caused due to the evaporation of a refrigerant flowing within tubes of tiny diameter. They employed numerous ANN configurations for training and selected the more precise one for thermal behavior. Their finding revealed the ability of ANN as a precise prediction tool for estimating the convective heat transmission amount. Ghahdarijani et al. [17] experimentally explored the nanofluids impact on the cooling performance and pressure drop of a jacked reactor by utilizing two distinct coolants nanofluids. Their experimental outcomes are implemented for ANN training and testing. Their study indicated a reasonable agreement between the experimental outcomes and that evaluated from the ANN algorithms. In their experiment, Bhowmik et al. [18] investigated the steady-state and transient heat transfers from a horizontal cylinder installed in a vertical circular duct under numerous Ra values and heat fluxes. They found that steady-state results matched positively with the obtainable outcomes in the literature. Besides, they found that the location of thermocouples affects the transfer of heat around the cylinder in a significant way. Bagheri et al. [19] analysed transportation of free convective energy in a C-shaped slanted compartment filled with a hybrid nanofluid and undergoing magnetic field and thermal flux. They implemented the finite element method and the ANN coupled with particles swarm optimization algorithm (PSO). They found ANN optimized by PSO algorithm to be more accurate at predicting the Nu than ANN alone. Abdelatief [20] evaluated the effect of free convection on a tube of an elliptical outer surface with multiple tilt angles and fluxes of heat, based on ANN and 3D ANSYS numerical computations. For identifying the appropriate ANN size, they used the Bayesian regularization algorithm as a backpropagation technique (BPT) approach. They correlated the experimental data and compare it with the ANN data output and showed a maximum deviation of ±13%. Recently, Parrales et al. [21] have been employed ANN to determine coefficients of heat transfer in every segment of a vertical double-pipe evaporator with helical section. Based on two ANN procedures, they suggested two empirical correlations for the Nu. They obtained each ANN model from the experimental outcomes, and in both ANN models they selected the LMA to determine the optimal magnitudes of the biases and weight. Their outcomes revealed the appropriateness of the ANN to determine Nu accurately. More recent published papers on ANN for radiative and convective heat transmission can be found in references [22–27].

To the best of the authors' knowledge, it is obvious from the above literature that there is no work in applying ANFIS for analyzing the free convection on a solid body under vacuum conditions. Hence, the present paper aims to experimentally investigate the characteristics of natural convection heat transfer from a solid cylindrical rod inside a vessel under vacuum conditions. The effect of vacuum pressure on the heat transfer rates from the heating element by convection and radiation is clarified. Also, the experimental results are utilized for ANFIS training which is employed to predict the problem heat transfer characteristics. The heat transmission predictions are performed for the solid rod under numerous heat fluxes for each vacuum pressure and the computed results are compared with that predicted from the ANFIS.

Experimental Apparatus

In the present study, an experimental apparatus consists of a pressure vessel containing a small heated element with a diameter (d = 6.15 mm) and length (L = 160 mm) suspended in the center. A thermocouple is fastened to the surface of the heater to quantity the temperature. Additionally, the vessel's interior is black, and it has a thermocouple mounted on its walls for measuring its temperature. Compressed air up to 1 bar (gauge) may be pumped into the vessel, or it can be emptied down to roughly 5 Pa (absolute). Data acquired can be extrapolated down to a complete vacuum (no convection), allowing the radiation-only transfer of heat to be isolated. Temperatures, pressures, and power supplied to the element are measured and displayed with instruments and a digital display. There are two pressure transducers on the apparatus, one for measuring pressures above atmospheric pressure and the other for measuring pressures below atmospheric pressure, which allow precise pressure and vacuum measurements. There is also a vacuum pump and a regulator to provide compressed air externally (up to 10 bar). The system contains a pressure relief valve, a photograph and schematic for the experimental apparatus are shown in Fig. 1a and Fig. 1b respectively.

(a)

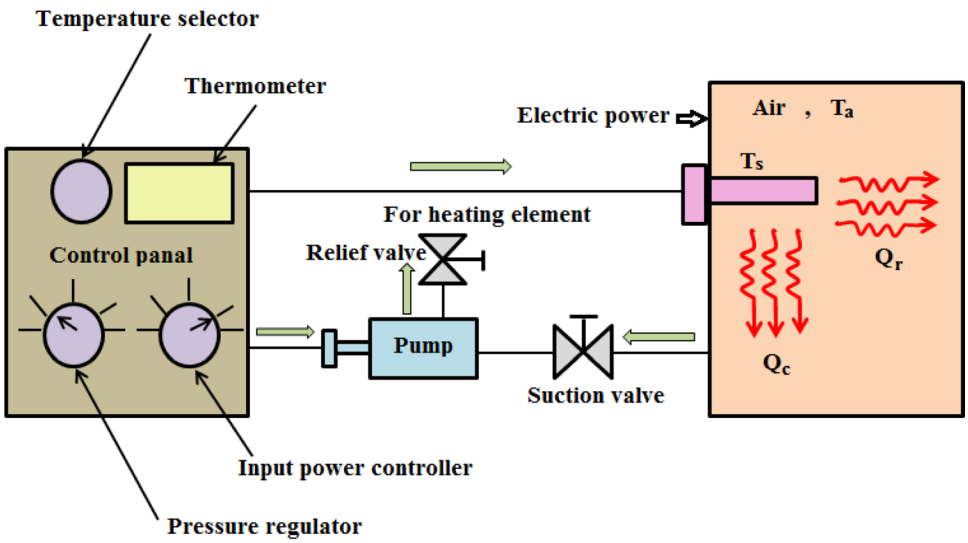

(b)

Fig. 1 **a**) Photograph for the testing apparatus, **b**) Schematic for the testing experimental apparatus

Heat Transfer Calculations

The relations of the heat transfer characteristics for the cylindrical heated rod are described. The total supplied energy to the bar can be evaluated as:

$$Q_S = 0.96IV \tag{1}$$

The value 0.96 represents the factor of power which equal to the cosine of the phase angle between the voltage and the current. The total heat transmitted from the bar to the surrounding can be expressed as:

$$Q = Q_r + Q_c \tag{2}$$

in which the heat transferred by convection from the bar to the air is given as:

$$Q_c = hA_s\left(T_s - T_a\right) \tag{3}$$

while the heat transferred by radiation from the bar is given as:

$$Q_r = \sigma A_s \varepsilon \left(T_s^4 - T_a^4\right) \tag{4}$$

Where σ is the Stephan-Boltzmann constant which is taken as ($\sigma = 5.67 \times 10^{-8}$ W m^{-2} K^{-4}) and ε is the emissivity which is taken as ($\varepsilon = 0.95$) [28]. Because the total supplied energy from the bar is the same as the total heat

transferred from the bar, then $Q = Q_S$, and by substituting Eqs. (3–4) into Eq. (2) and solving for the overall coefficient of heat transfer (h), the following relation will be obtained:

$$h = \frac{\left[\left(\frac{Q_S}{A_s}\right) - \sigma\varepsilon\left(T_s^4 - T_a^4\right)\right]}{\left(T_s - T_a\right)} \tag{5}$$

Consequently, the Nusselt number relation for natural convection and radiation can be obtained as below:

$$Nu = \frac{hd}{k} \tag{6}$$

The Grashof number (Gr) is a non-dimensional number in fluid dynamics and transfer of heat which relates the buoyancy force to the viscous force that exerts on a fluid. For air the Grashoff number (Gr) can be predicted from the following relation:

$$Gr = \frac{\beta g \theta_s \rho^2 d^3}{\mu^2} \tag{7}$$

where θ_s is the temperature difference between the bar surface temperature (T_s) and air temperature (T_a) which it is stated as below:

$$\theta_s = \left(T_s - T_a\right) \tag{8}$$

The thermo-physical properties of air in Eq. (7) are calculated at the mean temperature ($T_m = (T_s + T_a)/2$), which are stated as follows:

$$\beta = \frac{1}{T_m}, \rho = \frac{P}{RT_m} \tag{9}$$

where R is the gas constant for air which it taken as ($R = 287\ J\ kg^{-1}\ K^{-1}$), while the Prandtl number for air is estimated as:

$$\Pr = \frac{\mu C_P}{k} \tag{10}$$

Experimental Procedure

The experimental procedure was done by recording the vacuum pressure inside the vessel, and then the power input to the heating element rod is calculated from Eq. (1). After the steady-state period is achieved, the measurements of the heating element rod surface temperature (T_s) and the temperature of the air inside the vessel (T_a) are recorded. Twenty experiments are performed, in which four different pressures inside the vessel are used and for each pressure five different values for power input to the heating rod are used. For each experiment, the pressure inside the vessel and the temperature of the heating rod surface and the air temperature inside the vessel are recorded. The mean temperature of the air inside the vessel (T_m) is calculated, and the properties of the air are evaluated at the mean temperature. The total heat input to the heating rod and the heat transferred by radiation are calculated using Eqs. (1) and (4), respectively. The heat transferred by convection from the bar to the air and the overall heat transfer coefficient are calculated using Eqs. (3) and (5), respectively. Then Nusselt number, Grashof number and Prandtl number are calculated using Eqs. (6, 7 and 10) respectively. The same procedure of calculations is performed for the rest of the experiments. The data obtained from the calculations from all experiments are used for the Neural–Fuzzy model to predict the characteristics of the natural convective transfer of heat. A correlation for the empirical Nusselt (Nu_{emp}) for the natural convection from the hot rod surface is obtained as follows:

$$Nu_{emp} = 0.27(Gr.\Pr)^{0.28} \tag{11}$$

The scope of Grashof number utilized in Eq. (11) is ($200 < Gr < 2100$), while Prandtl number scope ($0.703 \le Pr \le 0.705$).

Neuro-Fuzzy Formulation

There are many strategies that treat the combination of fuzzy logic with a neural network. In this study, the Adaptive Neuro–Fuzzy Inference System (ANFIS) will be used which was implemented by Jang [29] and it was functionally equivalent to the fuzzy inference mechanism produced by Sugeno [30]. This method may be explained with the following numerical example of two rules as shown in Fig. 2.

Rule 1: if x in A_1 domain and y in B_1 domain then

$$z_1 = a_1 x + b_1 y + r_1 \tag{12}$$

Rule 2: if x in A_2 domain and y in B_2 domain then

$$z_2 = a_2 x + b_2 y + r_2 \tag{13}$$

In this study, four inputs are considered (T_s, T_a, Q, and P) and the object output is Nu. The rules for the present study can be written as:

Rule 1: if T_s in A_1 domain, T_a in B_1 domain, Q in C_1 domain and P in D_1 domain then

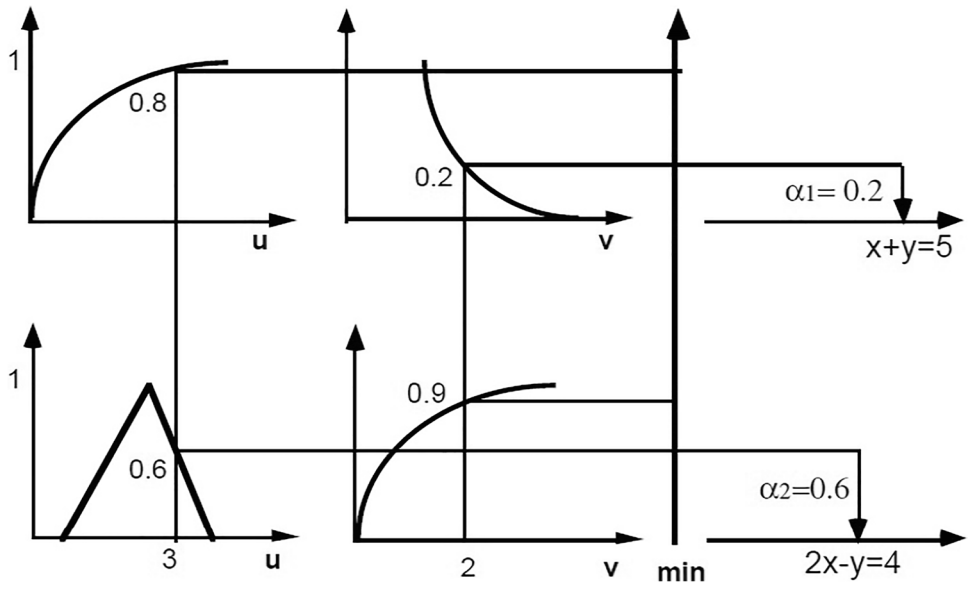

Fig. 2 Sugeno's inference mechanism [30]

$$z_1 = a_1 T_s + b_1 T_a + c_1 Q + d_1 P + r_1 \quad (14)$$

Rule 2: if T_s in A_2 domain, T_a in B_2 domain, Q in C_2 domain and P in D_2 domain then

$$z_2 = a_2 T_s + b_2 T_a + c_2 Q + d_2 P + r_2 \quad (15)$$

Rule 3: if T_s in A_3 domain, T_a in B_3 domain, Q in C_3 domain and P in D_3 domain then

$$z_3 = a_3 T_s + b_3 T_a + c_3 Q + d_3 P + r_3 \quad (16)$$

Rule 4: if T_s in A_4 domain, T_a in B_4 domain, Q in C_4 domain and P in D_4 domain then

$$z_4 = a_4 T_s + b_4 T_a + c_4 Q + d_4 P + r_4 \quad (17)$$

A hybrid neural net computationally identical to this type of reasoning which is shown in Fig. 3.

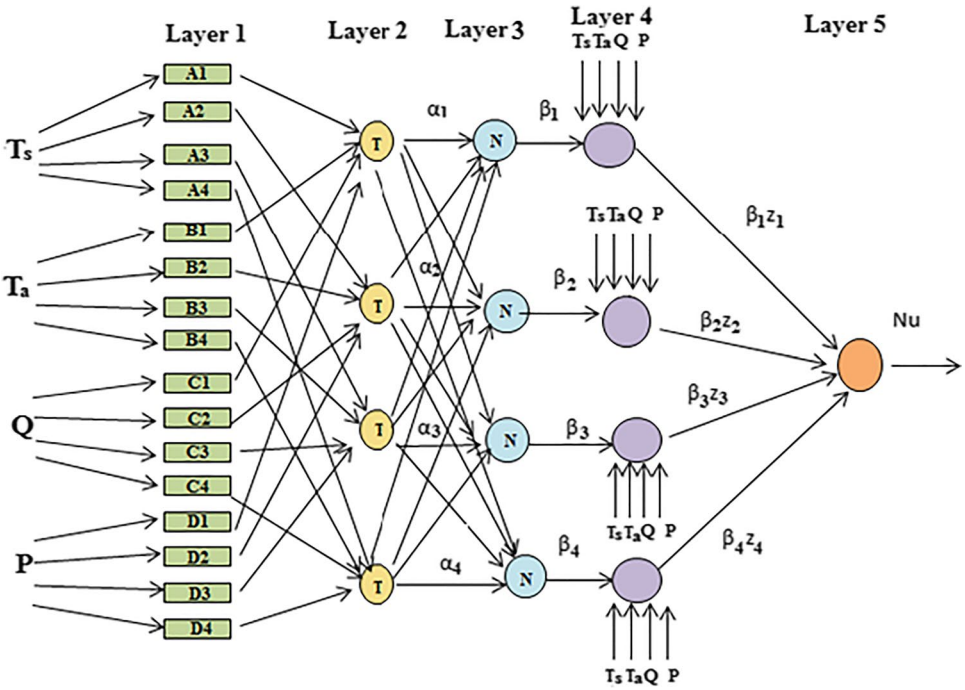

Fig. 3 General representation of ANFIS

In order to explain the methodology of the used technique, four rules and four linguistic values have been considered for every input. In the first layer, the signals of inputs are converted to degrees of memberships as shown in the Eq. (18).

$$\begin{aligned} A_i(T_s) &= e^{\left(\frac{-1}{2}((T_s-a_{i1})/b_{i1})^2\right)}, \\ B_i(T_a) &= e^{\left(\frac{-1}{2}((T_a-a_{i2})/b_{i2})^2\right)}, \\ C_i(Q) &= e^{\left(\frac{-1}{2}((Q-a_{i3})/b_{i3})^2\right)}, \\ D_i(P) &= e^{\left(\frac{-1}{2}((P-a_{i4})/b_{i4})^2\right)} \end{aligned} \tag{18}$$

The power of any rule is evaluated in the second layer of the ANFIS representation as it explained in Eqs. (19–22).

$$\begin{aligned} \alpha_1 &= A_1(T_s) \times B_1(T_a) \times C_1(Q) \times D_1(P) \\ &= A_1(T_s)\ \Lambda B_1(T_a) \Lambda C_1(Q) \Lambda\ D_1(P) \end{aligned} \tag{19}$$

$$\begin{aligned} \alpha_2 &= A_2(T_s) \times B_2(T_a) \times C_2(Q) \times D_2(P) \\ &= A_2(T_s)\ \Lambda B_2(T_a)\ \Lambda C_2(Q)\ \Lambda D_2(P) \end{aligned} \tag{20}$$

$$\begin{aligned} \alpha_3 &= A_3(T_s) \times B_3(T_a) \times C_3(Q) \times D_3(P) \\ &= A_3(T_s)\ \Lambda B_3(T_a)\ \Lambda C_3(Q)\ \Lambda D_3(P) \end{aligned} \tag{21}$$

$$\begin{aligned} \alpha_4 &= A_4(T_s) \times B_4(T_a) \times C_4(Q) \times D_4(P) \\ &= A_4(T_s)\ \Lambda B_4(T_a)\ \Lambda C_4(Q)\ \Lambda D_4(P) \end{aligned} \tag{22}$$

Then, the values of the rules' strength are normalized as they appear in Eqs. (23–26).

$$\varphi_1 = \frac{\alpha_1}{\alpha_1 + \alpha_2 + \alpha_3 + \alpha_4} \tag{23}$$

$$\varphi_2 = \frac{\alpha_2}{\alpha_1 + \alpha_2 + \alpha_3 + \alpha_4} \tag{24}$$

$$\varphi_3 = \frac{\alpha_3}{\alpha_1 + \alpha_2 + \alpha_3 + \alpha_4} \tag{25}$$

$$\varphi_4 = \frac{\alpha_4}{\alpha_1 + \alpha_2 + \alpha_3 + \alpha_4} \tag{26}$$

The product of the normalized firing level and the individual rule output any rule can be arranges as shown in Eqs. (27–30).

$$\varphi_1 z_1 = \varphi_1\left(a_1 T_s + b_1 T_a + c_1 Q + d_1 P + r_1\right) \tag{27}$$

$$\varphi_2 z_2 = \varphi_2\left(a_2 T_s + b_2 T_a + c_2 Q + d_2 P + r_2\right) \tag{28}$$

$$\varphi_3 z_3 = \varphi_3\left(a_3 T_s + b_3 T_a + c_3 Q + d_3 P + r_3\right) \tag{29}$$

$$\varphi_4 z_4 = \varphi_4\left(a_4 T_s + b_4 T_a + c_4 Q + d_4 P + r_4\right) \tag{30}$$

Finally, a single node in the fifth layer computes the overall system output (Nu) from the following relation:

$$\mathrm{Nu} = \varphi_1 z_1 + \varphi_2 z_{2+} \varphi_3 z_3 + \varphi_4 z_4 \tag{31}$$

Results and Discussion

The results of natural convection under vacuum conditions for a solid rod have been implemented with the four vacuum pressures P = 50.6, 60.6, 71.8, and 100.2 kPa, and a set of surface temperature (T_s) and ambient temperature (T_a) for each P value.

Fig. 4 shows the variation of Nu with Q at different pressures inside the vessel. From the figures, for constant pressure inside the vessel, Nu increases with increasing Q. This increment in Nu owing to increasing the buoyancy force which is resulted from increasing the surface temperature of the heating element. The percentage increase of Nu at P = 100.2 kPa is 5.87% within the scope of heat input variation.

Likewise, the figure exhibit that Nu decrease with decreasing the pressure inside the vessel owing to the lessen in the air mass inside which means reducing the convection heat transfer rate inside the vessel. The percentage reduction between the highest and lowest pressures in Nu at Q = 5 W is 42.2% for the pressure variation range inside the vessel.

Fig. 5 shows the variation of Q_r with Q at all studied pressures. The figure shows that the rate of Q_r increases with increasing Q due to the increase in the surface temperature of the heating element. The percentage increase in Q_r at P = 100.2 kPa is 152.82% within the scope of heat input variation. Also, the rate of Q_r ascends with decreasing the pressure inside the vessel due to a decrease in the convection heat transfer rate which is resulted from a reduction in the air quantity inside the vessel. The percentage ascend in radiation heat transmission rate between the highest and lowest pressures at Q = 11 W is determined as 21% within the pressure variation range inside the vessel.

Four significant factors are considered as inputs to predict the complex and important states of Nu (output) in the heat convection case study. These factors are Q (input1), T_s (input2), T_a (input3) and P (input4). There is no direct relation which related these inputs with the desired output therefore a most powerful intelligent technique named adapted neuro fuzzy inference system (ANFIS) is used in this investigation. This technique makes an effective combination of the ability to control fuzzy logic with the capability of prediction in the neural network. This method depends on the Sugeno

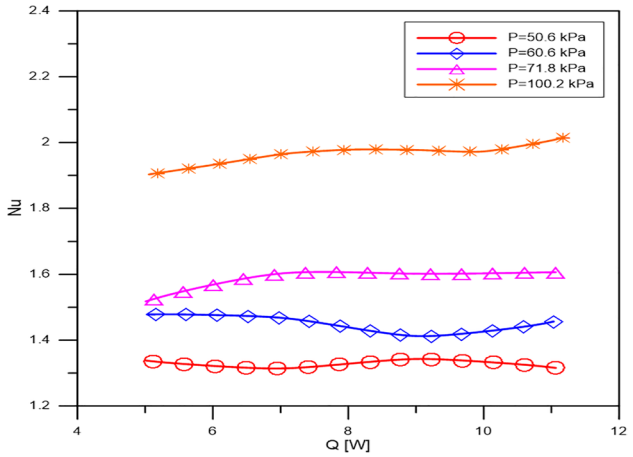

Fig. 4 Q vs. Nu at various pressures

inference system. The membership functions of the output in Sugeno may be considered linear or constant. While the inputs can be represented with any suitable function such as Gaussian, Triangular, Z-shaped, Trapezoidal, etc. However, in this study Gaussian membership function has been used and linear type is handled. This fact tends the output of ANFIS to adapt with linear behavior in the output space according to the variation of inputs. The linear dependency of the rules on the main parameters of the inputs makes ANFIS very acceptable for use as interpolating manipulator which can produce a linear behavior at different states of nonlinear models. This advantage of Sugeno has appeared a high efficiency in interpolating the magnitudes of Nu although the nonlinear behavior in some parts of device operation.

Three methods of ANFIS are used with the best optimization for their parameters. The first method has an ability of producing an inference engine of fuzzy system based on the division of the domain of fuzzy sets. It shows an acceptable result as shown in Fig. 6 where the fitting between the output of ANFIS and the experimental data can be noticed clearly in all testing samples. These results have been obtained after a hard training and the best selection of the type and number of memberships as shown in Figs. 7 and 8. In this type of ANFIS, two Gaussian memberships are considered and 40% testing samples with 60% training samples are chosen. However, these two memberships which are named as MF1and MF2 should include the whole range of the four inputs with normalized degree and main form parameters of magnitudes estimated based on the prediction strategies. Any membership contains a set of events or data which are collected with each other in some special properties which must not be found in the other groups of fuzzy sets. The initial step size is taken as 0.3 and according to the behavior of error, it is increased by multiplying it with a constant number of 1.5 while no decrease in the step size has been applied in this test due to the nature of testing data. The hard profile of Gaussian membership functions of input1 is changed after training to a smooth curve with a reduction of the degree of memberships from a range of [0–1] to another range of [0.5–1] which appears an adequate behavior with the variation of this input. In the same manner, the degree of membership for the input2 is changed after training to a new range of [0–0.5]. Also, for input3, the degree of membership is changed for the first membership to a range of [0–0.5] and the other to a range of [0.5–1]. However, this modification of the mathematical form of memberships is implemented by using some learning strategies which have high ability for estimating membership function parameters which are included with artificial neural network that is considered in ANFIS operation. Finally, with the input4, this degree is modified to a range of [0.5–1]. It can be concluded that the best selection of the main parameters of membership functions at using this adaptive technique is implemented due to the great ability of this method to represent the information in computerize device. That capability in treatment the train and test data has gave accurate interpolation through the

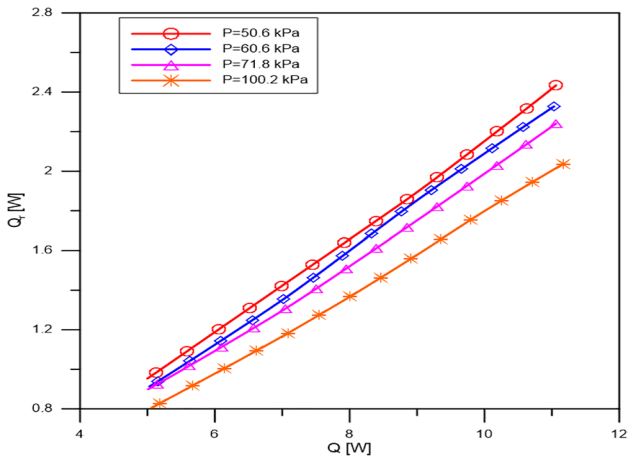

Fig. 5 Q vs. Q_r at various pressures

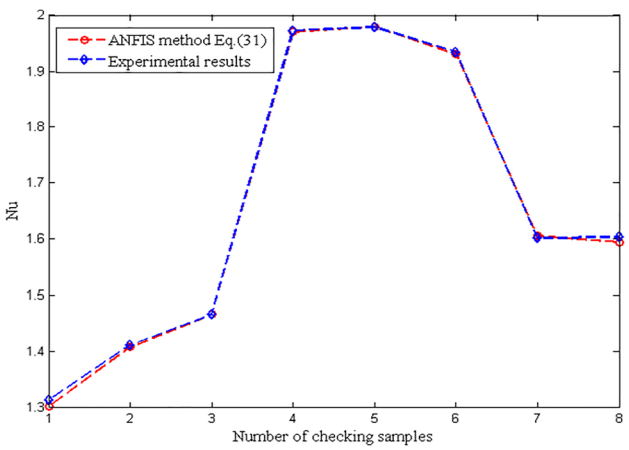

Fig. 6 Nu predicted by ANFIS (grid partition method)

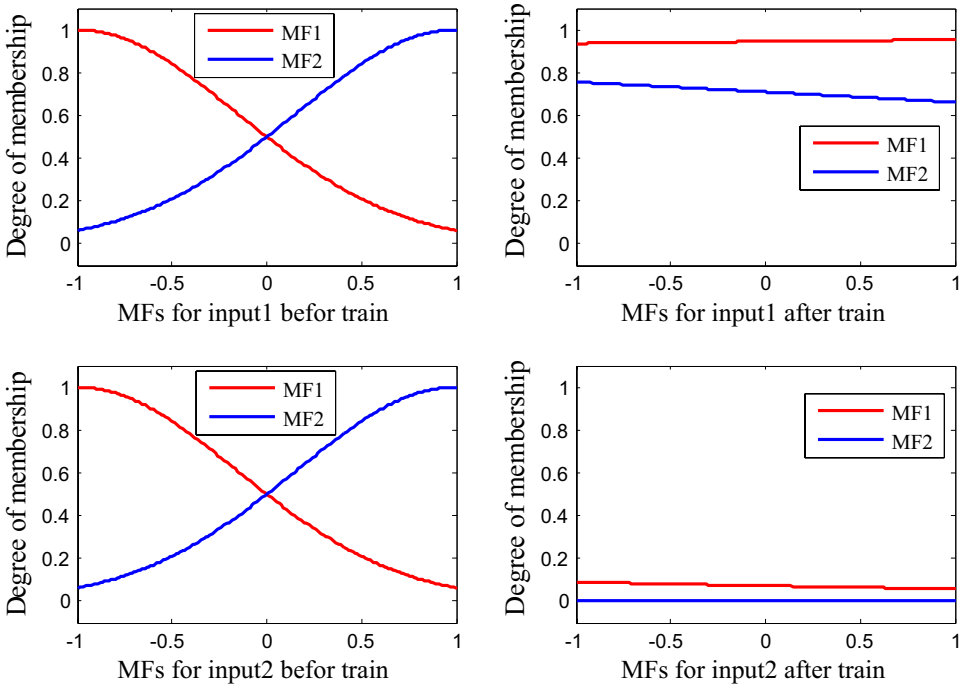

Fig. 7 Memberships of Q (input1) and T_s (input2) at using grid partition method

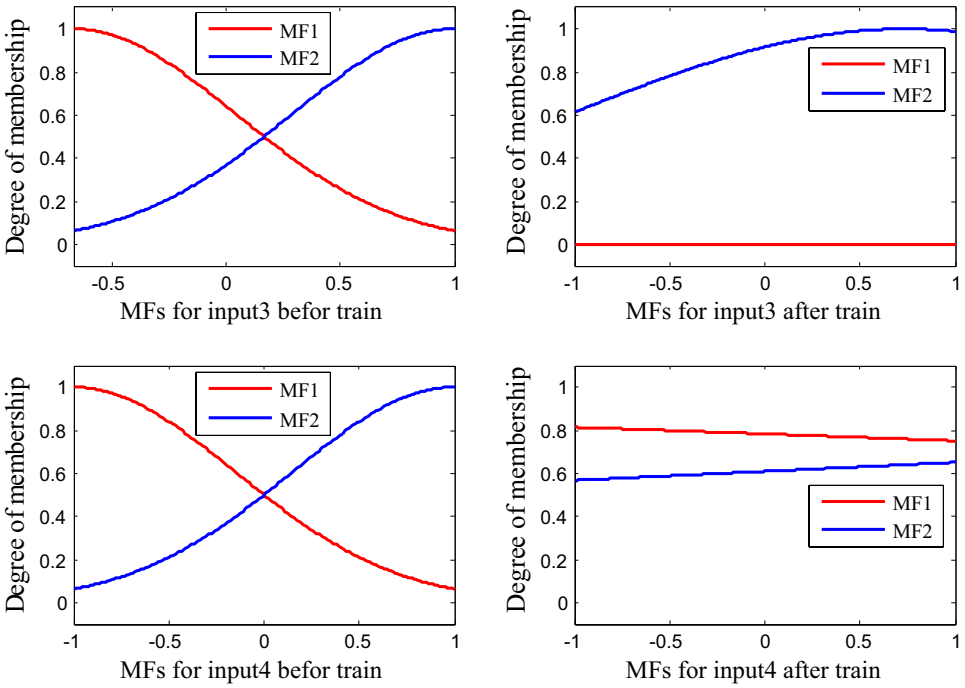

Fig. 8 Memberships of T_a (input3) and P (input4) at using grid partition method

erratic nature of some experimental samples. The presented method had appeared as a compact technique as shown in Fig. 6, even if the variation of T_s, T_a, Q and P was taken as complex and difficult manners.

In some applications of experimental data analyses, there is no clear opinion about the nature of these data. This fact means that estimating the number of membership functions that may classify the behavior of the operating system or a plant model is very useful and effective. So, a very powerful method depending on the subtractive clustering method is used in this study which can generate a number of clusters by estimating a suitable radius based on the differences between the selected centers and the given points of data. However, the selection of a small radius may lead to a large number of membership functions and then a large rule will be generated. Moreover, a great value of radius will lead to a

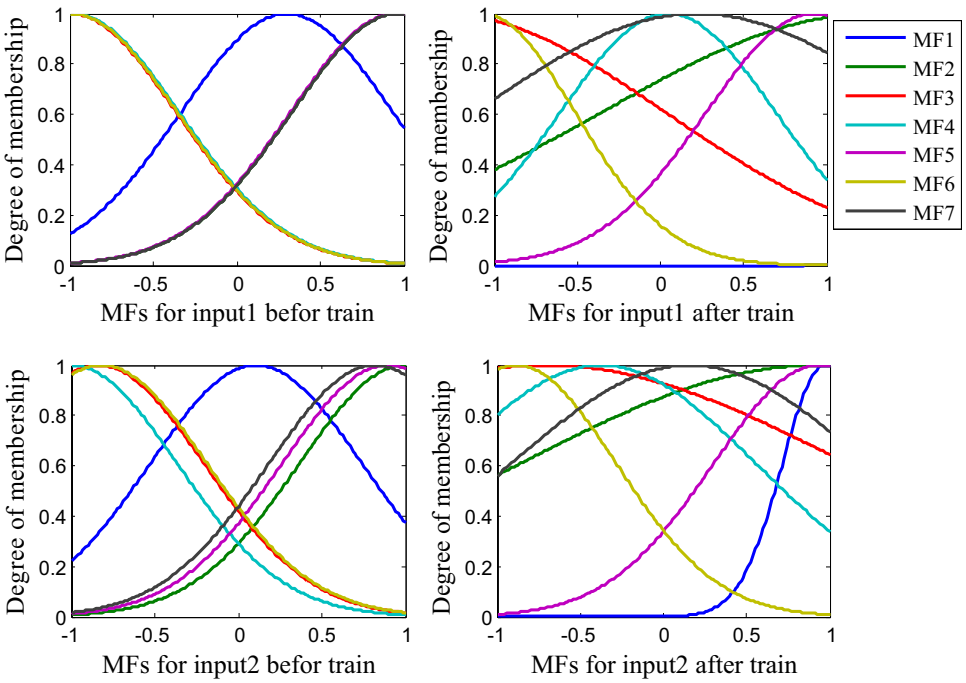

Fig. 9 Memberships of Q (input1) and T_s (input2) using subtractive clustering

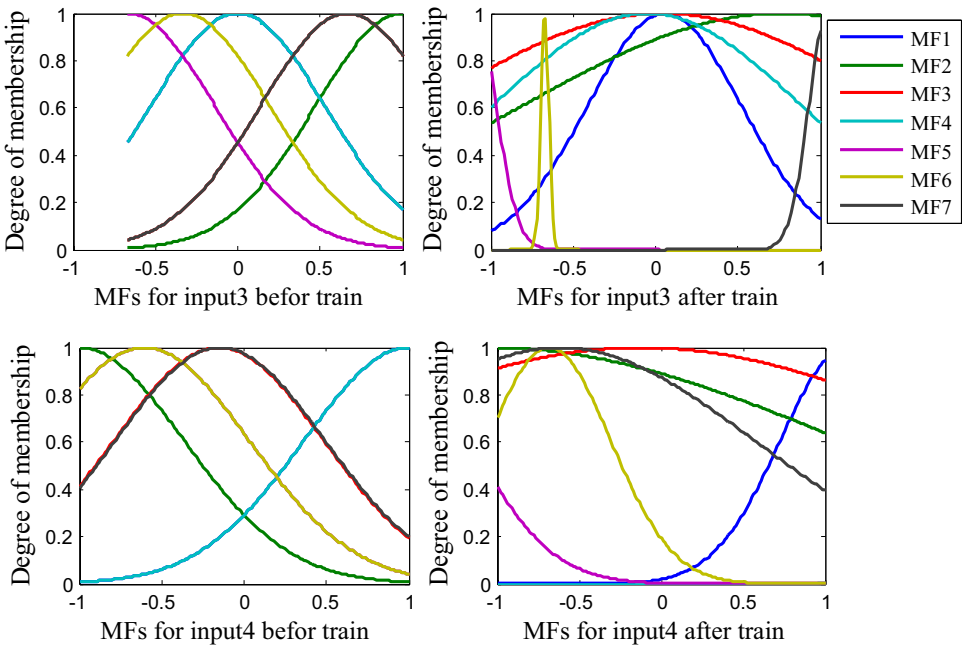

Fig. 10 Memberships of T_a (input3) and P (input4) using subtractive clustering

small number of membership functions and a small number of rules. In the present study, an optimization was implemented to reach the optimum value of the radius of clusters which is equal to 0.9.

This magnitude of radius had produced seven memberships (MF1, MF2, MF3, MF4, MF5, MF6 and MF7) for each input as shown in Fig. 9 (for Q and T_s) and Fig. 10 (for T_a and P). These memberships were trained by employing neural network technique in order to obtain the best formulation with suitable grade of memberships. This number of memberships is very difficult to be used by grid partition method because of the large number of rules that needed with this method. Therefore, subtractive clustering has produced an acceptable strategy of calculating Nu and applies the best role to reach an adequate behavior as it appears at the good agreement of the ANFIS output with the identical samples of the experimental set as portrayed in Fig. 11.

The absence of the idea about the number of membership functions and the nature of the data in each group of information led to consider a very effective method in this

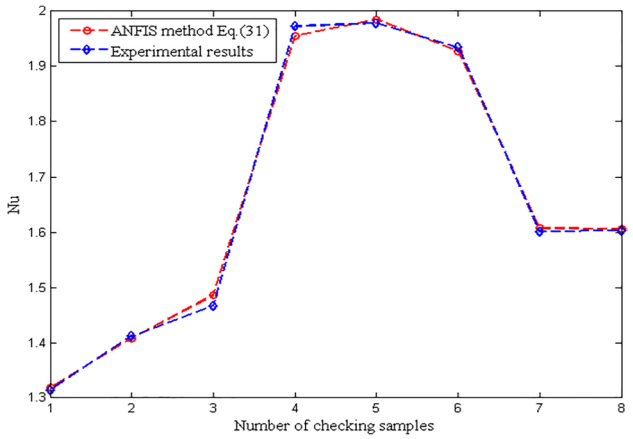

Fig. 11 Nu predicted by ANFIS subtractive clustering

study depending on selecting an initial guess for the centers of generated clusters. These centers will be trained with suitable optimization methods according to an adequate objective function in order to reach the optimum values of cluster's center in each collection of data. However, the main aim of the optimization schemes represents the magnitudes of the differences between the selected centers and the given points of data with a suitably weighted percent depending on the membership degree. This technique of clustering the data is named fuzzy C-mean clustering (FCM). After a sufficient iteration, a range of the suitable number of membership functions was obtained that may produce an acceptable behavior for the given experimental data of the presented work. This range is from (2) to (10) clusters with Gaussian type for inputs and linear for output. However, Fig. 12 shows the memberships of (Q) and (T_s) before and after the training step which uses an artificial neural network with number of clusters equal to (4) for each input. Also, Fig. 13 has appeared four membership functions (MF1, MF2, MF3 and MF4) for the (T_a) and (P) before and after training. It can be concluded clearly from the result shown in Fig. 14, that this method is very effective and suitable to relate four inputs with one output even though no specified model that represent this system or information. The best agreement of the output of ANFIS with the type of FCM as compared with experimental results is indicated in Fig. 14 which proves the high robustness and efficiency of this method in modeling input/output data of complex nature and erratic behavior.

The three methods of ANFIS are tested with different operating conditions and great variation in the effective parameters of each method. To demonstrate the accuracy and robustness of this intelligent technique, a comparison against some correlation approaches had been implemented as shown in Fig. 15. It can be observed from the results that the fuzzy expert knowledge with neural learning ability that formulated in ANFIS can realize satisfactory and good concordance with experimental testing data rather than that gained via conventional and classical correlation methods. The superiority of modeling input/output data using ANFIS for the present application of the heat case study had appeared clearly in Fig. 15, especially in samples' numbers 2, 4, 6 and 7. However, the ability of Sugeno inference system at the computational representation of data can maintain reasonably fitting with the desired outputs at a wide range of operational characteristics.

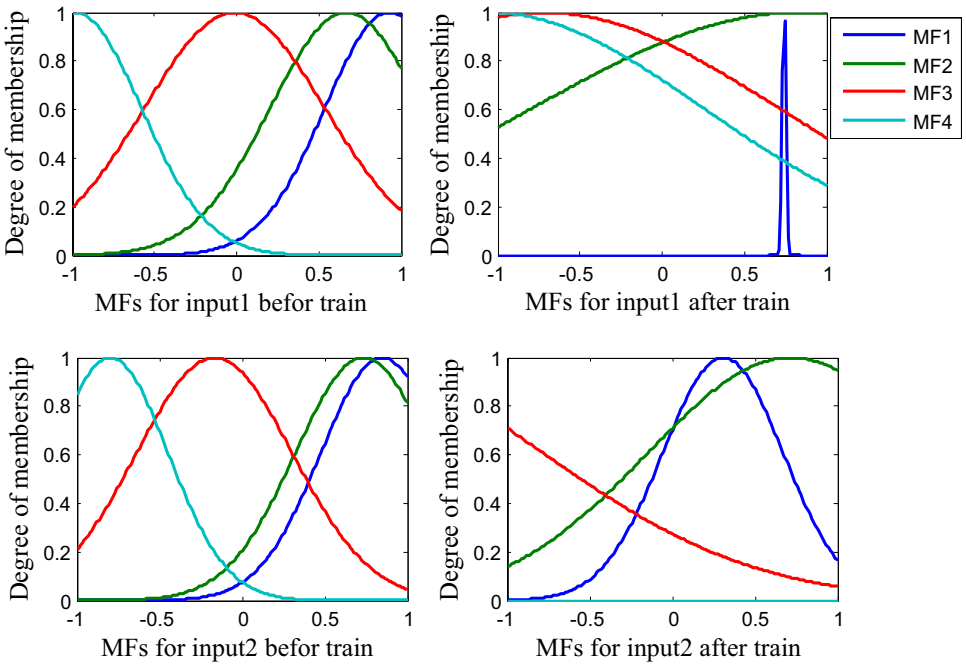

Fig. 12 Memberships of Q (input1) and T_s (input2) using fuzzy C-mean clustering (FCM)

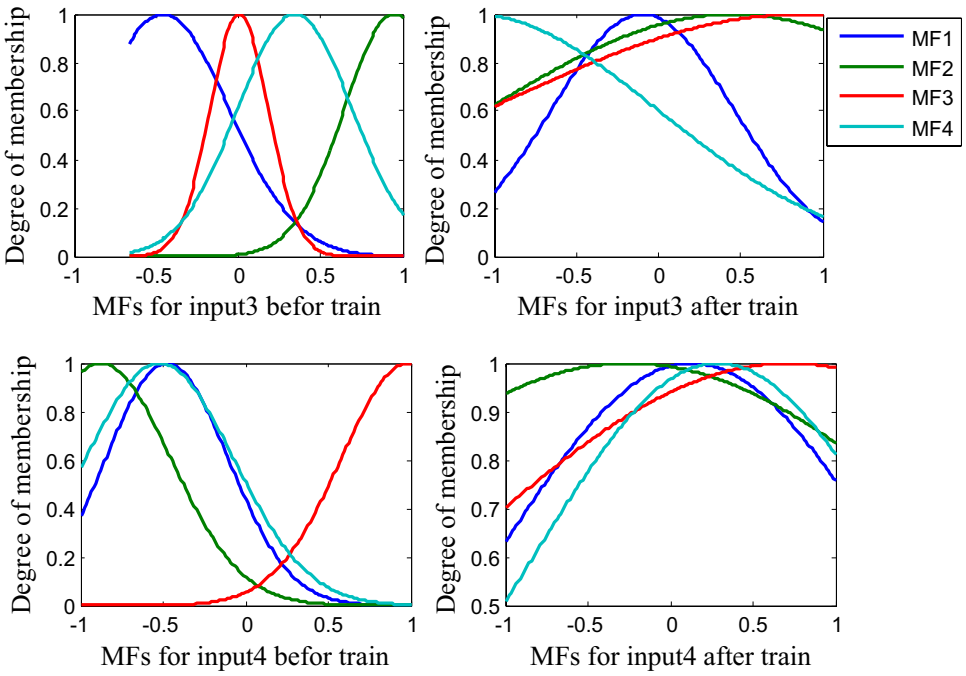

Fig. 13 Memberships of T_a (input3) and P (input4) using fuzzy C-mean clustering (FCM)

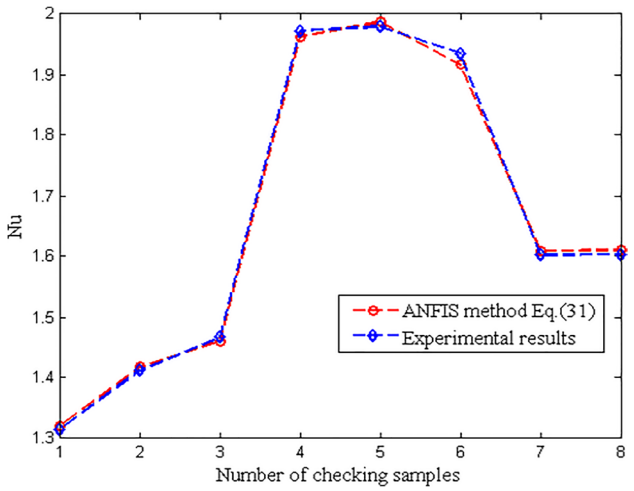

Fig. 14 Nu predicted by fuzzy C-mean clustering (FCM)

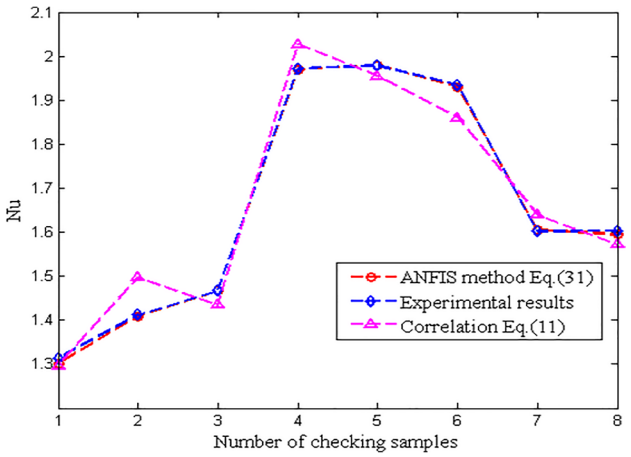

Fig. 15 Nu comparison between ANFIS and correlation results

Conclusions

The natural convection and radiation heat transfer from a solid cylindrical rod inside a closed vessel under vacuum conditions with the adaptation of ANFIS is examined. The following conclusions are obtained:

1. The reduction in pressure for constant heat flux increases the radiation heat transfer and decreases the natural convection heat transfer. Also, for constant pressure increasing the heat flux resulting in an ascend in the radiation heat transmission by approximately 25 times greater than that for natural convection.
2. For constant pressure inside the vessel, the variation of radiation heat transfer with input heat rate is steepest than that of the variation of natural heat transfer with input heat rate. Also, the variation of Q_r and Nu with pressure inside the vessel for constant heat input rate can be approximated as vertical parallel lines.
3. The results indicate that ANFIS can be represented as one of the best strategies for analyzing and studying the characteristics of natural convection and radiation heat transfers from a solid cylindrical rod inside a vessel under vacuum conditions.

4. The power of ANFIS in formulating a direct input–output relations may lead to producing an acceptable fitting with the experimental data as compared with classical correlation methods.
5. The optimization of the main parameters of ANFIS methods such as the number of membership functions in the grid partition method and the value of the radius of the cluster in the subtractive clustering method has a great effect on the modification of the performance of these methods.

Declarations

Competing Interests The authors did not receive support from any organization for the submitted work.

References

1. Ashjaee M, Afzali R, Niknami M, Amiri M, Yousefi T (2006) "Neural network analysis of free convection around isothermal elliptic tube," in *Proceedings of 8th Biennial ASME Conference on Engineering Systems Design and Analysis, ESDA2006*, vol. 2006, https://doi.org/10.1115/esda2006-95238
2. Hayati M, Yousefi T, Ashjaee M, Hamidi A, Shirvany Y (2007) Application of artificial neural networks for prediction of natural convection heat transfer from a confined horizontal elliptic tube. World Acad Sci 28:269–274
3. Atayilmaz ZÖ, Teke I (2009) Experimental and numerical study of the natural convection from a heated horizontal cylinder. Int Commun Heat Mass Transf 36(7):731–738. https://doi.org/10.1016/j.icheatmasstransfer.2009.03.017
4. Özgür Ataylmaz Ş (2010) Transient and steady-state natural convection heat transfer from a heated horizontal concrete cylinder. Int J Therm Sci 49(10). https://doi.org/10.1016/j.ijthermalsci.2010.05.019
5. Atayilmaz ŞÖ, Demir H, Ağra Ö (2010) Application of artificial neural networks for prediction of natural convection from a heated horizontal cylinder. International Communications in Heat and Mass Transfer 37(1):68–73. https://doi.org/10.1016/j.icheatmasstransfer.2009.08.009
6. Amiri A, Karami A, Yousefi T, Zanjani M (2012) Artificial neural network to predict the natural convection from vertical and inclined arrays of horizontal cylinders. Polish J Chem Technol 14(4):46–52. https://doi.org/10.2478/v10026-012-0101-6
7. Tahavvor AR, Yaghoubi M (2012) Analysis of natural convection from a column of cold horizontal cylinders using artificial neural network. Appl Math Model 36(7):3176–3188. https://doi.org/10.1016/j.apm.2011.10.003
8. Saravanakumar PT, Mayilsamy K, Boopathi Sabareesh V (2013) ANN modeling of forced convection solar air heater. Int Rev Model Simul 6(6). https://doi.org/10.1109/icctet.2013.6675911
9. Kayaci N et al (2013) Determination of the single-phase forced convection heat transfer characteristics of TiO2Nanofluids flowing in smooth and Micro-fin tubes by means of CFD and ANN analyses. Curr Nanosci 9(1):61–80. https://doi.org/10.2174/1573413711309010012
10. Zainuddin N, Hashim I, Ismoen M, Roslan R (2015) The effect of radiation on free convection from a heated horizontal circular cylinder. Appl Mech Mater 773–774:378–386. https://doi.org/10.4028/www.scientific.net/amm.773-774.378
11. Sebastian G, Shine SR (2015) Natural convection from horizontal heated cylinder with and without horizontal confinement. Int J Heat Mass Transf 82:325–334. https://doi.org/10.1016/j.ijheatmasstransfer.2014.11.063
12. Dey P, Sarkar A, Das AK (2015) Prediction of unsteady mixed convection over circular cylinder in the presence of nanofluid- a comparative study of ann and gep. J Nav Archit Mar Eng 12(1):43–56. https://doi.org/10.3329/jname.v12i1.21812
13. Dey P, Sarkar A, Das AK (2016) Development of GEP and ANN model to predict the unsteady forced convection over a cylinder. Neural Comput Appl 27(8):2537–2549. https://doi.org/10.1007/s00521-015-2023-8
14. Dey P, Das A (2015) Prediction of Unsteady Forced Convection over Square Cylinder in the Presence of Nanofluid by Using ANN. Int J Mech Mechatronics Eng 9(6). https://doi.org/10.5281/zenodo.1106931
15. Kamble LV, Pangavhane DR, Singh TP (2015) Artificial neural network based prediction of heat transfer from horizontal tube bundles immersed in gas-solid fluidized bed of large particles. J Heat Transf 137(1):1–9. https://doi.org/10.1115/1.4028645
16. Romero-Méndez R, Lara-Vázquez P, Oviedo-Tolentino F, Durán-García HM, Pérez-Gutiérrez FG, Pacheco-Vega A (2016) Use of artificial neural networks for prediction of the convective heat transfer coefficient in evaporative Mini-tubes. Ing Investig y Tecnol 17(1):23–34. https://doi.org/10.1016/j.riit.2016.01.003
17. Ghahdarijani AM, Hormozi F, Asl AH (2017) Convective heat transfer and pressure drop study on nanofluids in double-walled reactor by developing an optimal multilayer perceptron artificial neural network. Int. Commun. Heat Mass Transf. 84:11–19. https://doi.org/10.1016/j.icheatmasstransfer.2017.03.014
18. Bhowmik H, Faisal A, Al Yaarubi A, Al Alawi N (2018) Analyses of natural convection heat transfer from a heated cylinder mounted in vertical duct. Int J Mech Mechatronics Eng 12(3):213–218. https://doi.org/10.5281/zenodo.1315903
19. Bagheri H, Behrang M, Assareh E, Izadi M, Sheremet MA (2019) Free convection of hybrid nanofluids in a C-shaped chamber under variable heat flux and magnetic field: Simulation, sensitivity analysis, and artificial neural networks. Energies 12(14). https://doi.org/10.3390/en12142807
20. Abdelatief MA, Zamel AA, Ahmed SA (2019) Elliptic tube free convection augmentation: an experimental and ANN numerical approach. Int. Commun. Heat Mass Transf. 108:104296. https://doi.org/10.1016/j.icheatmasstransfer.2019.104296
21. Parrales A et al (2019) Heat transfer coefficients analysis in a helical double-pipe evaporator: Nusselt number correlations through artificial neural networks. Entropy 21(7):1–14. https://doi.org/10.3390/e21070689
22. Aylı E (2020) Modeling of mixed convection in an enclosure using multiple regression, artificial neural network, and adaptive neuro-fuzzy interface system models. Proc Inst Mech Eng Part C J Mech Eng Sci 234(15). https://doi.org/10.1177/0954406220914330
23. Cho HW, Park YG, Seo YM, Ha MY (2020) Prediction of the heat transfer performance of mixed convection in a lid-driven enclosure with an elliptical cylinder using an artificial neural network. Numer Heat Transf Part A Appl 78(2):29–47. https://doi.org/10.1080/10407782.2020.1777793
24. Kumar MKH, Vishweshwara PS, Gnanasekaran N (2020) Evaluation of artificial neural network in data reduction for a natural convection conjugate heat transfer problem in an inverse approach: experiments combined with CFD solutions.

Sadhana - Acad Proc Eng Sci 45(1):1–15. https://doi.org/10.1007/s12046-020-1303-x
25. Yarahmadi M, Mahan JR, McFall K (2020) Artificial neural networks in radiation heat transfer analysis. J Heat Transfer 142(9). https://doi.org/10.1115/1.4047052
26. Shoaib M et al (2021) Intelligent computing with Levenberg–Marquardt backpropagation neural networks for third-grade Nanofluid over a stretched sheet with convective conditions. Arab J Sci Eng. https://doi.org/10.1007/s13369-021-06202-5
27. Shafiq A, Çolak AB, Sindhu TN, Al-Mdallal QM, Abdeljawad T (2021) Estimation of unsteady hydromagnetic Williamson fluid flow in a radiative surface through numerical and artificial neural network modeling. Sci Rep 11(1). https://doi.org/10.1038/s41598-021-93790-9
28. Bergman DDPTL, Lavine AS, Incropera FP (2011) Fundamentals of heat and mass transfer, 7th ed. John Wiley & Sons, NJ
29. Jang JSR (1993) ANFIS: Adaptive-Network-Based Fuzzy Inference System. IEEE Trans Syst Man Cybern 23(3). https://doi.org/10.1109/21.256541
30. Burns RS (2001) Advanced control engineering, 1st ed. Elsevier, Butterworth-Heinemann, UK